

Coupled phase transformation, chemical decomposition, and deformation in plastic-bonded explosive: Simulations

Valery I. Levitas^{a)}

Department of Mechanical Engineering, Texas Tech University, Lubbock, Texas 79409, USA

Bryan F. Henson, Laura B. Smilowitz, David K. Zerkle, and Blaine W. Asay

Los Alamos National Laboratory, Los Alamos, New Mexico 87545, USA

(Received 30 June 2007; accepted 22 October 2007; published online 11 December 2007)

Numerical simulations of the heating with constant rate of a PBX (plastic-bonded explosive) 9501 formulation consisting of the energetic crystal HMX embedded in a polymeric binder inside of a rigid cylinder is performed. The continuum thermo-mechanochemical model of the behavior of a PBX 9501 developed in the preceding paper [V. I. Levitas, B. F. Henson, L. B. Smilowitz, D. K. Zerkle, and B. W. Asay, *J. Appl. Phys.* **102**, 113502 (2007)] is applied. The model describes the $\beta \leftrightarrow \delta$ phase transformations in crystalline HMX, chemical decomposition of the HMX and binder leading to gas formation, gas leaking from the cylinder, elastic, thermal, and transformational straining, as well as straining due to mass loss. We study the kinetics of the $\beta \leftrightarrow \delta$ phase transformations and pressure buildup, as well as how they are affected by the heating rate, initial porosity and prestrain, HMX and binder decomposition, and gas leaking rule. © 2007 American Institute of Physics. [DOI: 10.1063/1.2822096]

I. INTRODUCTION

The PBX 9501 formulation is an important high explosive with wide applications. It consists of 94.9% by weight of the organic energetic crystals HMX (octahydro-1,3,5,7-tetranitro-1,3,5,7-tetrazocine) embedded in a polymeric binder. The binder consists of 2.5% of Estane and 2.5% nitroplasticizer; we will neglect 0.1% of antioxidant. In the preceding paper,¹ a continuum thermo-mechanochemical model of the behavior of a PBX 9501 is developed and analyzed. The model describes the $\beta \leftrightarrow \delta$ phase transformations (PTs) in crystalline HMX, chemical decomposition of the HMX and binder leading to gas formation, gas leaking from the cylinder, elastic, thermal, and transformational straining, as well as straining due to mass loss. The kinetics model of the $\beta \leftrightarrow \delta$ PTs is fully physically based. It represents a combination of nucleation kinetics based on a suggested physical nucleation mechanism in HMX via melt-mediated nanocluster transformation^{1,2} and the growth kinetics based on virtual melting.^{1,3,4} This model describes well the temperature dependence of both the interface propagation velocity and volume fraction of the δ phase obtained in various experiments under isothermal conditions and zero pressure.^{5–8} Our goal is to study the $\beta \leftrightarrow \delta$ PTs numerically under complex pressure-temperature paths in which a constant temperature rate is prescribed and pressure variation is found from the solution of the mechanical problem. The equations for chemical decomposition of HMX and nitroplasticizer are the simplest phenomenological ones that allow us to solve this problem. They describe well the mass loss due to a solid-gas reaction step and ignore other steps in the solid and gas. Reaction heat is also neglected because the temperature is prescribed.

Mechanical theory is fully geometrically nonlinear and it correctly takes into account all finite and large strains. Application of the coupled thermo-mechanochemical model in numerical simulations of the above-mentioned processes allows us to reproduce pressure variation that affects the $\beta \leftrightarrow \delta$ PTs.

The paper is organized as follows. A complete system of equations which is used in our simulations is summarized in Sec. II. In Sec. III, the results of the simulation of coupled phase transformation, chemical decomposition, and deformation in PBX 9501 during heating inside of a rigid cylinder are presented. The effect of the heating rate, initial porosity and prestraining, HMX and binder decomposition, and gas leak rule on the kinetics of the $\beta \leftrightarrow \delta$ PT and pressure buildup is analyzed numerically. In Sec. IV, we demonstrate that application of our previous kinetic model⁹ for the PT in HMX based on a phenomenological nucleation kinetics has serious problems. Despite the fact that it describes isothermal experiments under zero pressure well, application of the model to the problem of PT in a rigid cylinder involving high pressure and eventual cyclic $\beta \leftrightarrow \delta$ PTs in the vicinity of the phase equilibrium line exhibits a number of contradictions. This shows the advantages of the fully physically based model developed in this paper. Section V contains the concluding remarks.

II. COMPLETE SYSTEM OF EQUATIONS

The following problem will be considered; see the scheme in Fig. 4 of Ref. 1. The cylindrical PBX 9501 sample is placed into a rigid cylinder and an initial macroscopic compressive strain ε_0 is prescribed by the piston motion. Then, the sample is heated with the heating rate h_r during which ε_0 is kept constant. The temperature is assumed to be

^{a)}Author to whom correspondence should be addressed. Electronic mail: valery.levitas@ttu.edu.

homogeneous. Pressure increases due to the thermal expansion. The Estane and nitroplasticizer melt in the temperature range 350–370 K. The gas in the initial voids is neglected. All initial voids are filled immediately by the binder as soon as it melts and any external pressure is applied. The pressure evolution and its effect on the $\beta \rightarrow \delta$ PT will be determined after the melting of the binder only. The simultaneous occurrence of the $\beta \rightarrow \delta$ PT and chemical decomposition of the nitroplasticizer and HMX will be considered. We neglected decomposition of the Estane. The gas which appears due to the HMX and binder decomposition partially remains as a new phase and partially disappears due to the leaking from the cylinder. It fills the voids that are created by decomposition of the HMX and binder and the initial voids that may still be left after melting of the binder and thermal expansion. The closed voids inside the HMX that are not accessible by the molten binder or gas will be neglected. The stress state in all constituents is hydrostatic. An assumption regarding homogeneous temperature is admissible for a slow heating rate and debatable under high heating rate. Such an assumption allows us to avoid the solution of a thermal heat conduction¹⁰ or coupled thermomechanical¹¹ boundary-value problem, and to study in an economic way the effect of various parameters on a constitutive (material) behavior for the $\beta \leftrightarrow \delta$ PTs within PBX 9501. The prescribed heating rate for the cylinder does not coincide with the heating rates in each material point due to the temperature heterogeneity and reaction heat. However, we may consider a small material volume near a thermocouple and chose external heating in a way that it provides the constant heating rate h_r . Then, temperature heterogeneity and reaction heat are not important. Because solid HMX is embedded in a liquid binder and/or gaseous medium, an assumption of homogeneous pressure is not very restrictive. Thus, our problem formulation allows us (1) to use simple and experimentally confirmed equations for chemical decomposition with neglected reaction heat and neglected reaction steps that are not important for the pressure buildup; (2) to avoid solution of the boundary-value problems; and (3) to perform multiparametric study of the $\beta \leftrightarrow \delta$ PTs within PBX 9501 under complex pressure-temperature paths.

Let us summarize the complete system of equations derived in Ref. 1, which describes coupled thermal expansion, chemical decomposition of the binder and HMX, $\beta \rightarrow \delta$ PT, gas leak, and elastic straining of the PBX 9501 sample into the rigid cylinder. All material parameters have been determined in Ref. 1.

Kinetics of the $\beta \leftrightarrow \delta$ PT:

$$\begin{aligned} \dot{c} &= bc(1-c); \\ c(t_0) &= c_0; \end{aligned} \quad (1)$$

$$\begin{aligned} b &= Z \frac{k\theta}{h} \exp\left(-\frac{\Delta h_{\delta \rightarrow m} + p\Delta v_{\delta \rightarrow m}}{R\theta}\right) \\ &\times \left[\exp\left(-\frac{\Delta g_{\beta \rightarrow \delta}}{R\theta}\right) - 1 \right]; \end{aligned} \quad (2)$$

$$\begin{aligned} t_0 &= \frac{\bar{t}_0}{\theta(t_0)} \exp \\ &\times \left(\frac{16\pi M^2 \Delta \gamma^3}{3\{\Delta s_{\beta \rightarrow \delta}[\theta(t_0) - \theta_e] - p(t_0, c_0)\Delta v_{\beta \rightarrow \delta}\}^2 \rho_h^2 k \theta(t_0)} \right); \end{aligned} \quad (3)$$

$$-\Delta g_{\beta \rightarrow \delta} = \Delta s_{\beta \rightarrow \delta}(\theta - \theta_e) - p\Delta v_{\beta \rightarrow \delta}. \quad (4)$$

Here, c is the volume fraction of the δ phase, t_0 is the nucleation time, c_0 is the volume fraction of an operational nucleus, θ is the temperature, p is the pressure, θ_e is the $\beta - \delta$ phase equilibrium temperature, $\Delta g_{\beta \rightarrow \delta}$, $\Delta s_{\beta \rightarrow \delta}$, and $\Delta v_{\beta \rightarrow \delta}$ are the change in the molar Gibbs potential, entropy, and volume during the $\beta \rightarrow \delta$ PT. $\Delta h_{\delta \rightarrow m}$ and $\Delta v_{\delta \rightarrow m}$ are the change in the molar enthalpy and volume during the melting of the δ phase; $M=0.296$ kg/mol is the HMX molecular weight, \bar{t}_0 and Z are pre-exponential factors, ρ_h is the mass density of HMX, $\Delta \gamma$ is the change in surface energy during nucleation via melt-mediated nanocluster transformation, $k = 1.381 \times 10^{-23}$ J/K and $h = 6.626 \times 10^{-34}$ J s are Boltzmann's and Planck's constants, respectively, and $R = 8.31$ J/(K mole) is the universal gas constants.

Equation (3) is a nonlinear algebraic equation for the nucleation time t_0 , which is evaluated starting with the instant when the PT criterion, $\Delta g_{\beta \rightarrow \delta} < 0$, is met. For the constant heating rate $\theta = \theta_i + h_r t$, where θ_i is the temperature at which the $\beta - \delta$ PT criterion is met, Eqs. (1) and (3) have to be substituted with

$$\begin{aligned} dc/d\theta &= bc(1-c)/h_r; \\ c(\theta_0) &= c_0; \end{aligned} \quad (5)$$

$$\Delta s_{\beta \rightarrow \delta}(\theta_i - \theta_e) = p(\theta_i)\Delta v_{\beta \rightarrow \delta}; \quad (6)$$

$$\frac{\theta_0 - \theta_i}{h_r} = \frac{\bar{t}_0}{\theta_0} \exp\left(\frac{16\pi M^2 \Delta \gamma^3}{3(\Delta s_{\beta \rightarrow \delta}(\theta_0 - \theta_e) - p(\theta_0, c_0)\Delta v_{\beta \rightarrow \delta})^2 \rho_h^2 k \theta_0}\right), \quad (7)$$

where Eqs. (6) and (7) are nonlinear algebraic equations for the determination of the temperatures θ_i and θ_0 at which the PT criterion and nucleation criterion are met for the first time.

Kinetic equation for the chemical decomposition of nitroplasticizer:

$$\begin{aligned} \dot{\phi}_{N/b} &= -k_N \phi_{N/b}; \\ k_N &= \exp(14.30) \exp\left(-\frac{9.623 \times 10^3}{\theta}\right); \\ \phi_{N/b}(0) &= 0.5. \end{aligned} \quad (8)$$

Here, $\phi_{N/b}$ is the mass fractions of the nitroplasticizer with respect to the initial total mass of the binder; its initial value is $\phi_{N/b}(0)=0.5$ and time is measured in seconds. For the constant heating rate, Eq. (8) can be integrated in the form

$$\phi_{N/b} = \phi_{N/b}(\theta_{in}) \exp \left\{ \frac{A}{h_r} \left[\exp \left(-\frac{B}{\theta_{in}} \right) \theta - \exp \left(-\frac{B}{\theta} \right) \theta + BEi \left(-\frac{B}{\theta_{in}} \right) - BEi \left(-\frac{B}{\theta} \right) \right] \right\}, \quad (9)$$

where $A = \exp(14.3) = 1.623 \times 10^6$, $B = 80\,000/R = 9622.5$ K, and $Ei(z) = -\int_{-\infty}^z e^{-t}/tdt$ ($z < 0$) is the exponential integral function.

Kinetic equation for the chemical decomposition of HMX:

$$\begin{aligned} \dot{f}_{hv} &= -k_h f_{hv} \{1 - f_{hv} \rho_h / [\rho_P(1 - f_{0v})]\}; \\ k_h &= 3.769 \times 10^9 \theta \exp \left(\frac{-150\,000}{R\theta} \right); \\ f_{hv}(0) &= f_{0hv} = 0.95(1 - f_{0v}) \rho_P / \rho_h, \end{aligned} \quad (10)$$

where f_{hv} is the current volume fraction of the HMX (the remaining unloaded volume of the HMX divided by the initial unloaded volume of the PBX), and ρ_P is the mass density of the void-free PBX, f_{0hv} is the initial volume fraction of HMX with respect to porous PBX, and f_{0v} is the initial volume fraction of voids in PBX.

Kinetic equation for the gas leaking from the cylinder:

$$\begin{aligned} \dot{\phi}_g^- &= 0 \quad \text{for } p \leq p_s; \\ \dot{\phi}_g^- &= 2.25 l J (p - p_s) \quad \text{for } p_s < p \leq 1.8 p_s; \\ \dot{\phi}_g^- &= l J p \quad \text{for } p \geq 1.8 p_s; \\ J &= \phi_g / f^* \quad \text{for } 0 \leq \phi_g \leq f^*; \\ J &= 1 \quad \text{for } \phi_g > f^*. \end{aligned} \quad (11)$$

Here, ϕ_g^- is the mass fraction of the gas (relative to the initial mass of the PBX) which leaked from the cylinder, ϕ_{gh} and ϕ_{gb} are the current mass fraction of the gas in the cylinder due to decomposition of the HMX and binder, respectively, $\phi_g = \phi_{gh} + \phi_{gb}$ is the total current mass fraction of the gas in the cylinder, p_s is the threshold pressure of the gas above which leaking is possible, l is the choked leak rate coefficient, and J is a function defined in the last line of Eq. (11) with $f^* = 10^{-3} - 10^{-4}$. For a constant heating rate, the time derivative in Eqs. (10) and (11) has to be substituted with the temperature derivative, and the right-hand part of the kinetic equations has to be divided by h_r .

The mass fraction of the gas in the cylinder:

$$\phi_g = 0.5(L_g + |L_g|); \quad (12)$$

$$\begin{aligned} L_g &= (0.5 - \phi_{N/b})0.05 + \left(0.95 - \frac{f_{hv} \rho_h}{\rho_P(1 - f_{0v})} \right) - \phi_g^- \\ &= \phi_{gb} + \phi_{gh}. \end{aligned} \quad (13)$$

The mass fraction of the gas in the cylinder due to decomposition of the nitroplasticizer and HMX, respectively:

$$\phi_{gb} = \phi_g \frac{(0.5 - \phi_{N/b})0.05}{(0.5 - \phi_{N/b})0.05 + \{0.95 - (f_{hv} \rho_h) / [\rho_P(1 - f_{0v})]\}}; \quad (14)$$

$$\phi_{gh} = \phi_g \frac{0.95 - (f_{hv} \rho_h) / [\rho_P(1 - f_{0v})]}{(0.5 - \phi_{N/b})0.05 + \{0.95 - (f_{hv} \rho_h) / [\rho_P(1 - f_{0v})]\}}; \quad (15)$$

Pressure in the cylinder:

$$p = \frac{HK_b K_h + \sqrt{H^2 K_b^2 K_h^2 + 4QS}}{2S}; \quad (16)$$

$$S = F_{hi} K_b + F_{bi} K_h;$$

$$H = F_{hi} + F_{bi} - F_0 / (1 - f_{0v});$$

$$Q = \left(\frac{\phi_{gh}}{M_{gh}} + \frac{\phi_{gb}}{M_{gb}} \right) R \theta \rho_P; \quad (17)$$

$$F_{hi} = F_h^\theta F_h^t F_h^m f_{0h};$$

$$F_{bi} = F_b^\theta F_b^m f_{0b}. \quad (18)$$

Here, $K_h = 15$ GPa and $K_b = 3.65$ GPa are, respectively, the bulk moduli of the HMX crystal and binder, F_h and F_b are the volumetric deformation gradients in the HMX and binder, the superscripts θ , t , and m designate the thermal and transformational components of the deformation gradients, as well as the component due to the mass loss during the chemical decomposition, $F_0 = 1 + \varepsilon_0$ is the deformation gradient that determines precompression in the PBX in the rigid cylinder due to piston motion, f_{0h} and f_{0b} are, respectively, the initial volume fractions of the HMX and binder with respect to void-free PBX, F_{hi} and F_{bi} are inelastic deformation gradients in the HMX and the binder, and M_{gh} and M_{gb} are the molecular masses of gas product due to the decomposition of the HMX and nitroplasticizer (it is assumed that $M_{gh} = M_{gb} = 0.037$ kg/mole). For the case $M_{gh} = M_{gb}$ considered in the paper, one gets $Q = (\phi_g / M_{gh}) R \theta \rho_P$ and there is no need to separate ϕ_g into ϕ_{gh} and ϕ_{gb} and use Eqs. (14) and (15).

Deformation gradients in the HMX and binder:

$$F_h^m = \varepsilon_h^m + 1;$$

$$F_h^t = \varepsilon_h^t + 1;$$

$$F_h^\theta = \varepsilon_h^\theta + 1;$$

$$F_b^m = \varepsilon_b^m + 1;$$

$$F_b^\theta = \varepsilon_b^\theta + 1, \quad (19)$$

where ε designate corresponding strains defined below.

Thermal expansion strains for the HMX and binder:

$$\varepsilon_h^\theta = c \varepsilon_\delta^\theta + (1 - c) \varepsilon_\beta^\theta = \varepsilon_\beta^\theta + c(\varepsilon_\delta^\theta - \varepsilon_\beta^\theta); \quad (20)$$

$$\varepsilon_b^\theta = 13.1 \times 10^{-5} (\theta - 300);$$

TABLE I. Thermodynamic properties for β - δ phase transformation and melting of β and δ phases. The parameters participating in the kinetic equation for the β - δ phase transformation are in bold.

	Δh (kJ/mole)	θ_e (K)	Δs (J/mole K)	$\Delta v^* 10^5$ (m ³ /mole)	ε'
β - δ	9.8	432	22.68	1.264	0.08
δ - m	69.9	550	127.09	1.066	0.067
β - m	79.7	532	149.77	2.330	0.147

$$\varepsilon_{\delta}^{\theta} - \varepsilon_{\beta}^{\theta} = 0.4 \times 10^{-5}(\theta - 432); \quad (21)$$

$$\varepsilon_b^{\theta} = 6 \times 10^{-5}(\theta - 300). \quad (22)$$

The strains in the nitroplasticizer (binder) and HMX due to mass loss during the chemical decomposition:

$$\varepsilon_b^m = \varepsilon_N^m = (0.5 - \phi_{N/b})\rho_b/\rho_N;$$

$$\varepsilon_h^m = f_{hv}/f_{0hv} - 1. \quad (23)$$

Here, ρ_N and ρ_b are the mass density of the nitroplasticizer and binder and we neglected decomposition of the Estane. All material parameters that have not been given above are enumerated in Tables I-IV.

III. SIMULATION OF COUPLED PHASE TRANSFORMATION, CHEMICAL DECOMPOSITION, AND DEFORMATION IN PBX 9501 FORMULATION

In this section we present results of the solution of the system of Eqs. (1)–(23) using the MATHEMATICA program.¹² Each of the kinetic equations, Eqs. (9) and (10), for the chemical decomposition of the nitroplasticizer and HMX are independent of pressure and of all other equations. They can be solved independently and used as input data for all other equations. At the first step, Eqs. (11)–(23) are solved without PT equations ($c=0$) to determine the corresponding pressure evolution. Then, the algebraic Eq. (6) is solved for the temperature θ_i at which the PT criterion is satisfied for the first time. As the next step, setting $c=c_0$ and recalculating the pressure, the algebraic Eq. (7) is solved for the θ_0 at which the nucleation criterion is met for the first time. Thus, for $\theta < \theta_0$, solution of Eq. (11)–(23) is used for $c=0$. Then, the complete system of Eqs. (1)–(23) is solved for $\theta_0 < \theta \leq 510$ K (the highest temperature of interest) using the previous solution at $\theta = \theta_0$ as the initial data. The pressure has a jump at $\theta = \theta_0$ due to the introduction of a finite concentration of operational nuclei and corresponding transformation strain.

Special care has to be taken while solving the nonlinear algebraic Eq. (7). Since the driving force for the PT, $-\Delta G_{\beta \rightarrow \delta}$, is squared in Eq. (7), there are two solutions corresponding to the positive (correct solution) and negative

TABLE II. Parameters in the kinetic equations for β - δ phase transformation.

Z	\bar{t}_o (s)	$\Delta\gamma$ (J/m ²)	c_0
7×10^{-13}	4.5×10^{-4}	4.78×10^{-4}	0.016

(unphysical solution) driving force. For a specific nonmonotonic pressure variation, Eq. (7) may have several solutions with the positive driving force; only the solution with the lowest temperature corresponds to the nucleation. Also, this equation contains an extremely fast-growing exponential function; during the iterative solution of Eq. (7) it can numerically diverge. Several methods can be used to improve the numerical procedure:

- An initial trial temperature, θ_{tr} , to start an iterative procedure can be taken as 0.5 to 1 K larger than the solution of the phase equilibrium condition $\Delta s_{\beta \rightarrow \delta}(\theta - \theta_e) = p(\theta, c_0)\Delta v_{\beta \rightarrow \delta}$ for pressure evaluated with the existing nucleus, i.e., for $c=c_0$;
- In addition to the solution of Eq. (7), solving the equation with the logarithm of the left and right part of Eq. (7) and comparing solutions;
- Checking that $\Delta G_{\beta \rightarrow \delta}[\theta_0, p(\theta_0, c_0)] < 0$;
- Substituting the solution back in Eq. (7) to be sure that the residual is negligible.
- Analyzing the graphical solution of Eq. (7) in order to avoid some unexpected situations.

The heating rates of interest are $h_r=0.1, 0.5, 1, 2, 5, 10$, and 20 K/min and will be used in all examples below. The solutions depend on the following parameters: $F_0/(1-f_{0v}) \approx 1 + \varepsilon_0 + f_{0v}$ that combines the prestraining F_0 and an initial porosity f_{0v} ; rate of heating h_r ; threshold for the gas leaking p_s and gas leaking coefficient l . The main features of the interaction between all thermo-chemomechanical processes in a rigid cylinder will be analyzed based on the following modeling examples.

(1) A typical case with $l=10^{-6}$ kg/(m³s MPa), $p_s = 10$ MPa, and $F_0/(1-f_{0v})=0.01$ (for example, $\varepsilon_0=-0.005$ and $f_{0v}=0.015$) will be considered in detail. The evolution of typical strains for $h_r=0.5$ and 20 K/min is shown in Fig. 1. The positive strains (those that lead to the pressure increase) are the thermal strain of the HMX $\varepsilon_h^{\theta}f_{0hv}$ (linear function in θ) and the transformation strain of HMX $\varepsilon^t f_{0hv}$, which is proportional to c and characterizes the PT kinetics. The thermal strain of the binder, $\varepsilon_b^{\theta}f_{0b}$, is 28 times smaller than the thermal strain of HMX and is not shown. The negative strains (those that lead to the pressure decrease) are the initial constant strain $-(\varepsilon_0 + f_{0v})$, strain in the HMX due to mass loss $\varepsilon_h^m f_{0hv}$ (which characterizes the HMX decomposition kinetics), and strain in the binder due to the mass loss of the nitroplasticizer (which characterizes the nitroplasticizer decomposition kinetics) $\varepsilon_N^m f_{0b}$. To observe the actual contribution of each strain, it is multiplied by the volume fraction of the corresponding component. The initial constant strain is taken with the negative sign because it is external (prescribed) strain rather than internal strains like all others. Indeed, compressive (negative) strain ε_0 increases pressure, while compressive (negative) internal stresses ε_N^m and ε_h^m cause the pressure to decrease.

For $h_r=0.5$ K/min, strain related to the mass loss of the nitroplasticizer appears at 380 K, intensively grows till 450 K, and remains constant ($\varepsilon_N^m f_{0b} = -0.5 \times 0.071 = -0.0355$) after the nitroplasticizer disappears at 462 K. The $\beta \rightarrow \delta$ PT starts at 440 K; there is a jump in the transformation strain

TABLE III. Initial mass and volume fractions of the PBX constituents.

f_{moh}	f_{moN}	f_{moE}	f_{oh}	f_{oN}	f_{oE}	f_{ob}
0.95	0.025	0.025	0.928	0.033	0.039	0.072

$\varepsilon^t f_{ohv} c_0 = 0.0012$ due to the appearance of the nucleus of the δ phase. The volume fraction of the δ phase and transformation strain grow very intensively until the pressure approaches the phase equilibrium line. In the temperature range 450–480 K, the volume fraction growth rate is approximately constant, after which growth is accelerated until completing the PT at 502 K. Maximum transformation strain after complete PT is $\varepsilon^t f_{ohv} = 0.08 \times 0.914 = 0.073$. Around 458 K, HMX decomposition starts and accelerates with the temperature growth; the maximum strain $|\varepsilon_h^m|/f_{ohv}$ exceeds 0.1. Acceleration in PT kinetics is related to acceleration in HMX decomposition that provides free volume for transformation expansion due to PT.

For the maximum heating rate $h_r = 20$ K/min, all kinetic processes are delayed and far from completion. Thus, strain related to the mass loss of the nitroplasticizer appears at 400 K and is about -0.02 at 510 K. HMX decomposition starts at 475 K and the corresponding strain is only -0.002 at 510 K. PT starts at 486.7 and reaches $c = 0.145$ and strain 0.01 at 510 K.

The corresponding pressure evolution is presented in Fig. 2. The lower the heating rate is, the earlier the pressure starts to build up and reach the leaking threshold $p_s = 10$ MPa. The pressure increase is mostly due to the decomposition of the nitroplasticizer in the closed volume. For larger temperature and the slowest heating rate of 0.1 K/min, pressure is just above the threshold p_s until the δ phase nucleation temperature 438.7 K, i.e., the rate of leaking is much higher than the rate of the nitroplasticizer decomposition. The higher the heating rate is, the larger the gas production with respect to leaking, the pressure increase above the threshold p_s , and the higher the δ phase nucleation pressure and temperature are. The maximum in the pressure curves before nucleation is related to the complete disappearance of the nitroplasticizer (and consequently the lack of the gas supply) while gas leaking is strong due to high pressure. The δ -phase nucleation is accompanied by the jumplike increase in pressure followed by a slight pressure decrease and then a sharp pressure increase. Then, for each h_r pressure evolves along (but slightly below) the phase equilibrium line, caused by the dynamic equilibrium between the volume decrease due to gas leaking and the volume increase due to the PT. When the $\beta \rightarrow \delta$ PT is completed (for $h_r = 0.1$ and 0.5 K/min), the pressure drops sharply due to a lack of transformation expansion. Then, the pressure grows for both these heating rates because of the intensification of the HMX decomposition with increasing temperature. For h_r

$= 0.1$ K/min and $\theta > 505$ K, the gas production due to the HMX decomposition is smaller than the gas leaking and pressure reduces again.

The PT kinetics is presented in Fig. 3 for all heating rates under study. The slower the heating rate is, the more complete the PT progress is. For $h_r = 0.1$ K/min and $h_r = 0.5$ K/min the PT is completed and for $h_r = 1$ K/min it is almost completed. Fast initial transformation progress for $h_r = 0.1$ –1 K/min is related to the pressure being significantly lower than the phase equilibrium pressure. Slower kinetics for $h_r = 0.1$ –1 K/min for higher temperatures as well as for all higher heating rates is related to the heating-loading path in the vicinity of the phase equilibrium line. Sharp acceleration of the $\beta \rightarrow \delta$ PT for $h_r = 0.1$ –1 K/min and high temperatures is due to the volume decrease due to the intense HMX decomposition and gas leaking (providing the space for transformation expansion), as well as due to high θ .

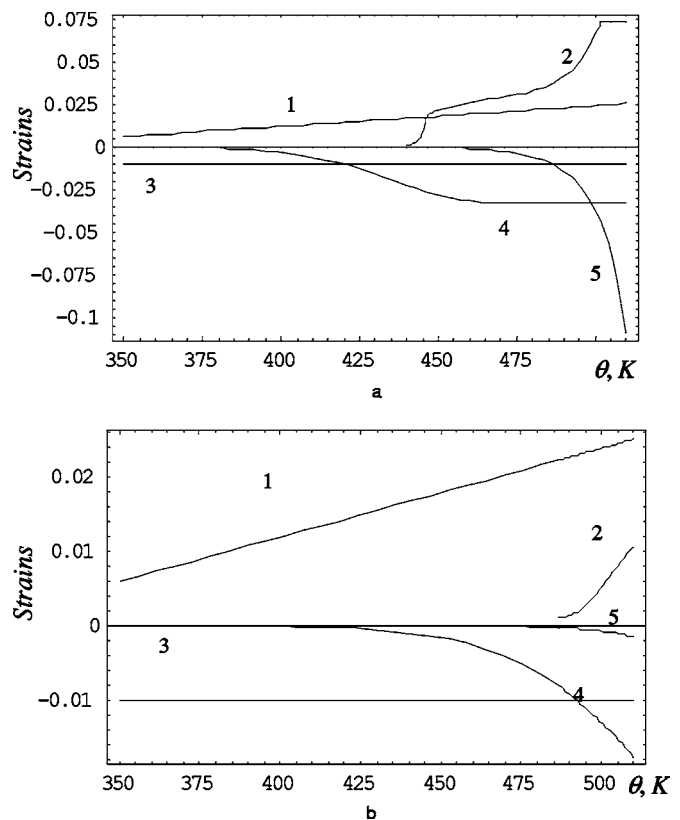


FIG. 1. Evolution of the main strain contributions for $l = 10^{-6}$ kg/(m³s MPa), $p_s = 10$ MPa, $F_0/(1-f_{0v}) = 0.01$ and (a) for the heating rate $h_r = 0.5$ K/min and (b) 20 K/min. The positive strains (those that lead to the pressure increase) are (1) the thermal strain of the HMX $\varepsilon_h^t f_{ohv}$ (linear function in θ) and (2) the transformation strain of HMX $\varepsilon^t f_{ohv}$, which is proportional to c and characterizes the PT kinetics. The negative strains (those that lead to the pressure decrease) are (3) the initial constant strain $-(\varepsilon_0 + f_{0v})$; (4) strain in the HMX due to mass loss $\varepsilon_h^m f_{ohv}$ (which characterizes the HMX decomposition kinetics); and (5) strain in the binder due to the mass loss of the nitroplasticizer (which characterizes the nitroplasticizer decomposition kinetics) $\varepsilon_N^m f_{0b}$.

TABLE IV. Mass densities of the PBX constituents (in kg/m³).

ρ_h	ρ_N	ρ_E	ρ_b	ρ_P
1905	1390	1190	1282	1860

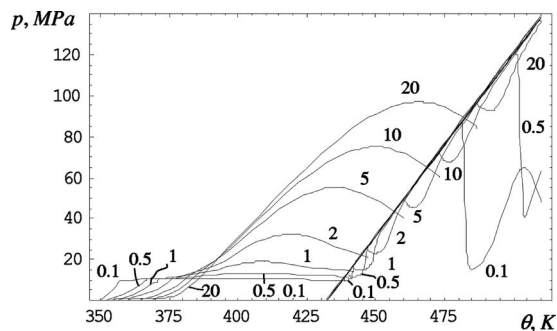


FIG. 2. Pressure evolution in a cylinder for $l=10^{-6}$ kg/(m³s MPa), $p_s=10$ MPa, $F_0/(1-f_{0v})=0.01$ and various heating rates (shown in K/min near the curves). The straight line is the β - δ phase equilibrium line.

Various contributions to the gas production in and flow from the cylinder are shown in Fig. 4. For $h_r=0.5$ K/min, the nitroplasticizer starts to decompose around 350 K and ends decomposition around 462 K. Just above 360 K the pressure exceeds the leaking threshold p_s and practically the entire gas completely leaks. HMX decomposition starts at 458 K and again the gas leaks almost completely till 502 K. At this temperature the $\beta \rightarrow \delta$ PT is completed and pressure drops. This decelerates the gas leaking and some product of HMX decomposition remains in the cylinder.

For $h_r=20$ K/min, all gas production and leaking activities are reduced by an order of magnitude. The nitroplasticizer and HMX start to decompose around 400 and 475 K, respectively. At 510 K, the mass fraction of gas due to the nitroplasticizer and HMX decomposition is 0.012 and 0.002 only. The maximal value of the mass fraction of the remaining gas in the cylinder is also 0.002 only at 510 K.

Note that the mass fraction of produced gas is $f_{gb}+f_{gh} = \phi_g + \phi_g^-$, i.e., it can be obtained in Fig. 4 by combining either of two corresponding curves.

(2) For all the same parameters but $l=10^{-9}$ kg/(m³s MPa), PT does not start below 510 K for any heating rate under study because of high gas pressure. The same happens for $l=10^{-8}$ kg/(m³s MPa) for $h_r=0.5$ –20 K/min; for $h_r=0.1$ K/min, the volume fraction of the δ phase reaches 0.1 but at further heating the δ phase disappears.

For $l=10^{-7}$ kg/(m³s MPa), PT does not start for $h_r=10$ and 20 K/min, and it starts at 506 K for $h_r=5$ K/min.

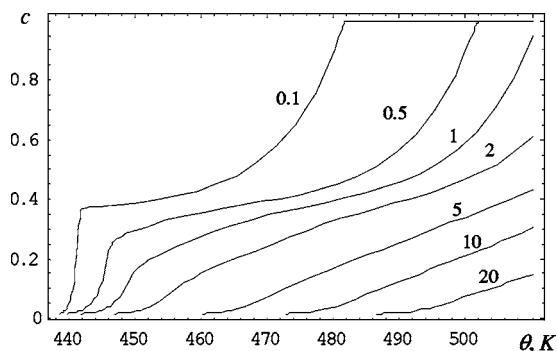


FIG. 3. Evolution of the volume fraction of the δ phase in a cylinder for $l=10^{-6}$ kg/(m³s MPa), $p_s=10$ MPa, $F_0/(1-f_{0v})=0.01$ and various heating rates (shown in K/min near the curves).

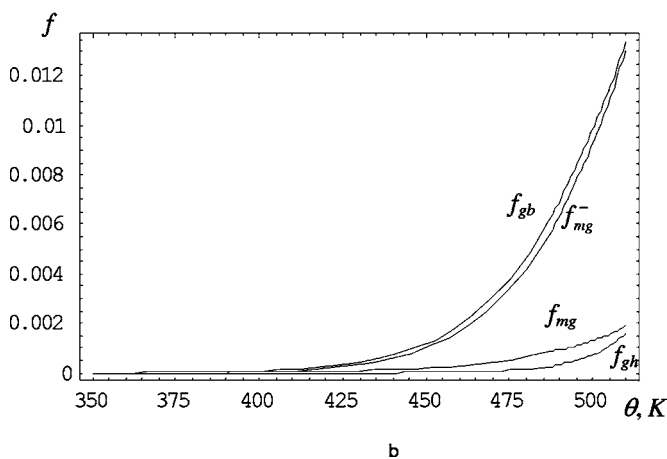
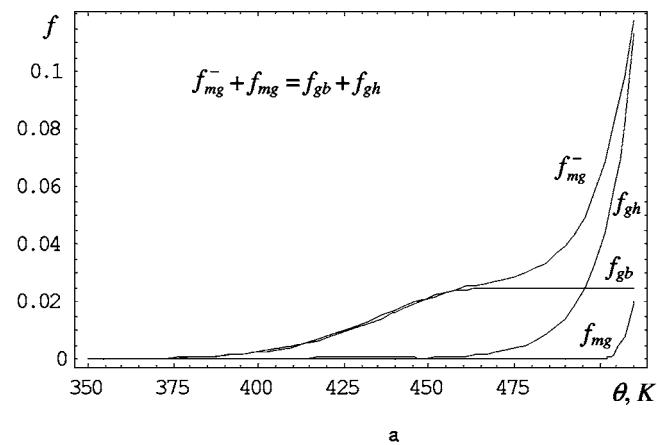


FIG. 4. Temperature variation of mass fraction of the nitroplasticizer decomposition, f_{gb} , HMX decomposition, f_{gh} , of gas leaking from the cylinder, ϕ_g^- , and remaining in the cylinder, ϕ_g for (a) $h_r=0.5$ K/min and (b) $h_r=20$ K/min. Other parameters are $l=10^{-6}$ kg/(m³s MPa), $p_s=10$ MPa, and $F_0/(1-f_{0v})=0.01$. The mass fraction of produced gas is $f_{gb}+f_{gh}=\phi_g + \phi_g^-$, i.e., it can be obtained by combining either of two corresponding curves.

For $h_r=0.1$ K/min (Figs. 5 and 6), the kinetics of PT is initially nearly the same as for $l=10^{-6}$ kg/(m³s MPa), including completing the PT at 482 K. However, slower leaking during the intense HMX decomposition above 494 K leads to a pressure increase and, in combination with the fast PT kinetics at high temperature, leads to complete reverse PT into the β phase. For $h_r=0.5$ K/min, the PT kinetics is suppressed in comparison with the case of $l=10^{-6}$

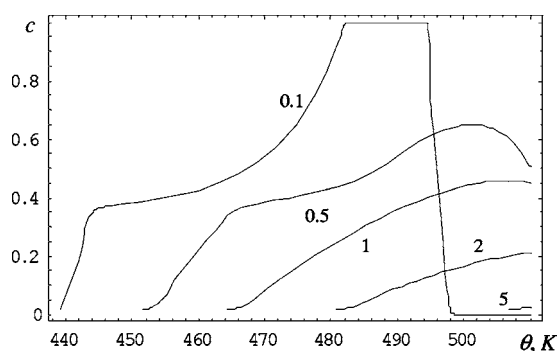


FIG. 5. Evolution of the volume fraction of the δ phase in a cylinder for $l=10^{-7}$ kg/(m³s MPa), $p_s=10$ MPa, $F_0/(1-f_{0v})=0.01$ and various heating rates (shown in K/min near the curves).

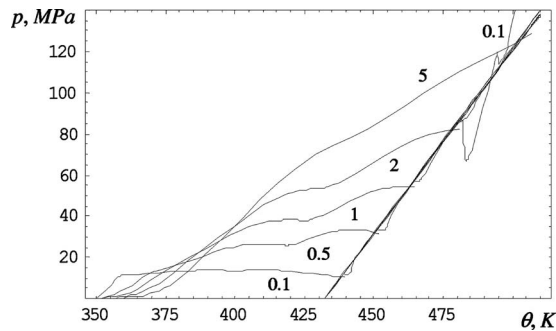


FIG. 6. Pressure evolution in a cylinder for $l=10^{-7}$ kg/($\text{m}^3\text{s MPa}$), $p_s=10$ MPa, $F_0/(1-f_{0v})=0.01$ and various heating rates (shown in K/min near the curves). The straight line is the β - δ phase equilibrium line.

kg/($\text{m}^3\text{s MPa}$); the volume fraction of the δ phase does not exceed 0.65 [instead of complete PT for $l=10^{-6}$ kg/($\text{m}^3\text{s MPa}$)] and then reduces to 0.5 at 510 K. A similar suppression of PT progress is observed for $h_r=1$ and 2 K/min but without the reverse PT.

(3) To model the conditions with no leaking, we set $p_s=1000$ MPa. The gas pressure grows drastically in this case and for $F_0/(1-f_{0v})=0.01$ and any heating rate between 0.1 and 20 K/min, pressure curve crosses the phase equilibrium line in the range 557–564 K. This is far beyond the temperature of interest and validity of our model, i.e., the $\beta \rightarrow \delta$ PT is completely suppressed for $\theta \leq 510$ K.

To reduce the gas pressure, we increased $F_0/(1-f_{0v})=0.03$ (for example, by increasing the initial porosity to $f_{0v}=0.035$). For a low heating rate in the range 0.1 to 2 K/min the PT was suppressed at the temperatures of interest below 510 K. For $h_r=5, 10,$ and 20 K/min, the evolution of the volume fraction of the δ phase and pressure is shown in Figs. 7 and 8. The larger h_r is, the earlier the PT starts, and the larger c is. This is opposite to the case with a gas leaking. In the case with a gas leaking, the main factor suppressing the $\beta \rightarrow \delta$ PT is the short time for PT (rather than gas pressure), which reduces with the increase in h_r . For the sealed cylinder, the main suppressing factor is the gas pressure, which (along with the gas production) decreases with increasing h_r . The volume fraction of the δ phase is quite small (less than 0.16 for the highest heating rate) and the pressure during the PT is close to the phase equilibrium line (Figs. 7 and 8).

For the larger porosity of $f_{0v}=0.055$ [$F_0/(1-f_{0v})=0.05$]

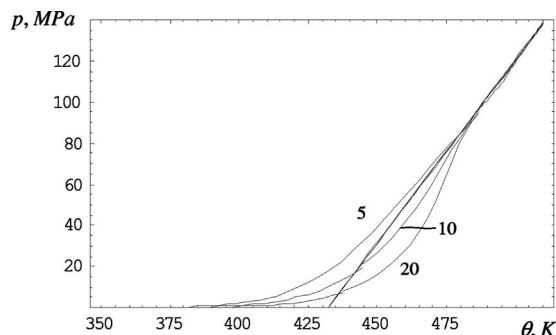


FIG. 7. Pressure evolution in a cylinder for no gas leaking and $F_0/(1-f_{0v})=0.03$ and various heating rates (shown in K/min near the curves). The straight line is the β - δ phase equilibrium line.

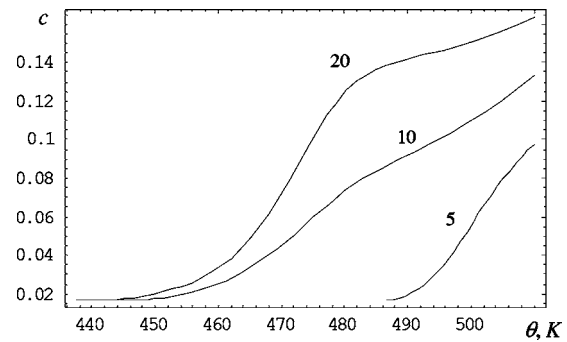


FIG. 8. Evolution of the volume fraction of the δ phase in a cylinder for no gas leaking and $F_0/(1-f_{0v})=0.03$ and various heating rates (shown in K/min near the curves).

and $h_r=0.1$ K/min, the PT was not observed below 510 K. For all other heating rates, c at 510 K grows with increasing h_r (Fig. 9). However, in some intermediate temperature ranges from 448 to 470 K and from 448 to 475 K, c for the heating rate of 20 K/min is smaller than for 5 K/min and 10 K/min, respectively. Also, for 0.5 and 1 K/min, direct $\beta \rightarrow \delta$ PT is followed by the reverse $\delta \rightarrow \beta$ PT due to a sharp gas pressure increase at high temperatures; for $h_r=0.5$ K/min, the δ phase completely disappears at 502 K. The pressure-temperature trajectory for $h_r=5$ to 20 K/min penetrates quite deep in the region of stability of the δ phase (Fig. 10), causing the intense $\beta \rightarrow \delta$ PT in the range 460–475 K. At higher temperature they approach close to the phase equilibrium line suppressing the PT. For 0.5 and 1 K/min, pressure trajectory returns back in the region of stability of the β phase causing the reverse PT.

(4) The opposite limit case with complete gas leaking was modeled by setting $p_s=0$ and $l=0.1$ kg/($\text{m}^3\text{s MPa}$); we also used $F_0/(1-f_{0v})=0.01$ (see Figs. 11 and 12). For $h_r=1$ to $h_r=20$ K/min, the initial pressure was zero until the touching between PBX 9501 and the cylinder which occurs due to the thermal expansion of PBX 9501 in the range 382–387 K. The pressure grows, reaches a maximum, and reduces, because the volume decrease due to the decomposition of the nitroplasticizer exceeds the thermal expansion. For $h_r=1$ K/min, the pressure reduces to zero and increases when touching between the PBX 9501 and cylinder occurs due to the intense $\beta \rightarrow \delta$ PT. For $h_r=5$ to $h_r=20$ K/min, the pressure and volume fraction c variations are very close to

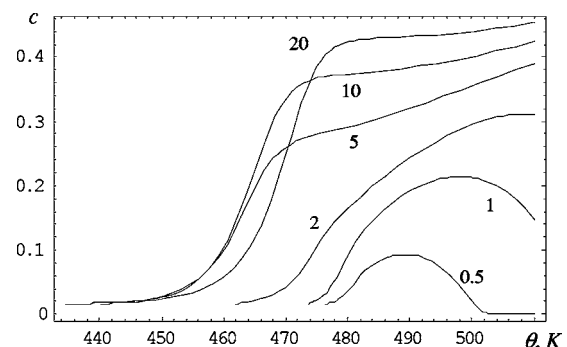


FIG. 9. Evolution of the volume fraction of the δ phase in a cylinder for no gas leaking and $F_0/(1-f_{0v})=0.05$ and various heating rates (shown in K/min near the curves).

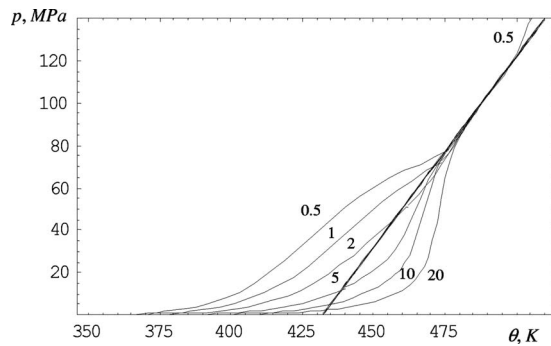


FIG. 10. Pressure evolution in a cylinder for no gas leaking and $F_0/(1-f_{0v})=0.05$ and various heating rates (shown in K/min near the curves). The straight line is the β - δ phase equilibrium line.

those for $p_s=10$ MPa and $l=10^{-6}$ kg/(m³s MPa) (Figs. 2 and 3). For $h_r=0.5$ and 1 K/min, the pressure is zero until the touching between PBX and the cylinder which occurs due to intense $\beta \rightarrow \delta$ PT in the range 432–435 K. In fact, for any heating rates the volume fraction of the δ phase for the cases with $p_s=0$ and $l=0.1$ kg/(m³s MPa) and with $p_s=10$ MPa and $l=10^{-6}$ kg/(m³s MPa) are very similar and shifted by approximately 5 K. The threshold p_s is important for $h_r=0.1$ and 0.5 K/min only. This means that for $p_s=10$ MPa and $l=10^{-6}$ kg/(m³s MPa) the gas phase in a cylinder does not play an important role; direct contact between solid PBX and a cylinder creates the major part of the pressure that affects the PT kinetics.

Summarizing, one can derive the following methods to control the $\beta \rightarrow \delta$ PT: It can be completely or partially suppressed by high pressure. Pressure can be increased by decreasing the initial porosity and gas leaking coefficient l and increasing the preliminary compression ε_0 and the threshold pressure p_s . The effect of the heating rate depends on the other parameters chosen. Thus, when the main suppressing factor is the gas pressure (for example, for small initial porosity and slow leaking), then an increase in h_r leads to a smaller amount of the produced gas and a smaller pressure, which promotes the PT. In the opposite case when the gas pressure is not important (for example, for large initial porosity and intense leaking), an increase in h_r directly suppresses the kinetics of the $\beta \rightarrow \delta$ PT, i.e., provides less time for $\beta \rightarrow \delta$ PT.

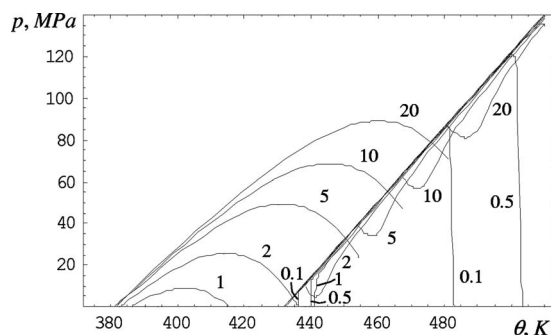


FIG. 11. Pressure evolution in a cylinder for complete gas leaking [$l=0.1$ kg/(m³s MPa), $p_s=0$, $F_0/(1-f_{0v})=0.01$] and various heating rates (shown in K/min near the curves). The straight line is the β - δ phase equilibrium line.

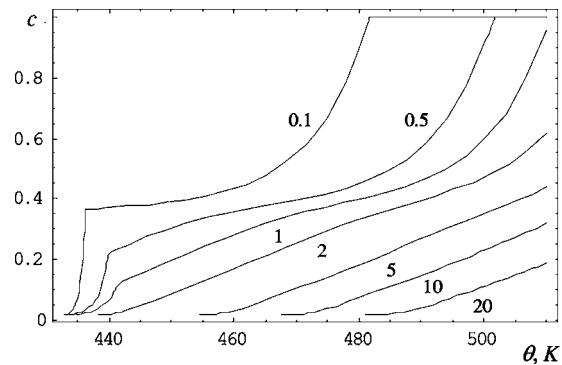


FIG. 12. Evolution of the volume fraction of the δ phase in a cylinder for complete gas leaking [$l=0.1$ kg/(m³s MPa), $p_s=0$, $F_0/(1-f_{0v})=0.01$] and various heating rates (shown in K/min near the curves).

Despite the fact that the parameters characterizing the gas leaking are not known, we found the main ranges of their effect. Thus, p_s of the order of 10 MPa does not affect the $\beta \rightarrow \delta$ PT significantly since the pressure in most cases is significantly higher. For $F_0/(1-f_{0v})=0.01$ the case with complete leaking [$p_s=0$ and $l=0.1$ kg/(m³s MPa)] and with $p_s=10$ MPa and $l=10^{-6}$ kg/(m³s MPa) are very similar for any heating rate because the gas phase in a cylinder does not play an important role for both cases; direct contact between solid PBX and a cylinder creates the major part of the pressure that affects the PT kinetics. For $l < 10^{-8}$ kg/(m³s MPa), there is no PT, and for 10^{-7} kg/(m³s MPa) the PT occurs for slow heating only. The case with no leaking depends significantly on $F_0/(1-f_{0v})$, with no PT for $F_0/(1-f_{0v})=0.01$ and intense PT for $F_0/(1-f_{0v})=0.05$.

IV. APPLICATION OF PHENOMENOLOGICAL NUCLEATION KINETICS

Here, we discuss the possibility of the application of our previous kinetic model for the $\beta \rightarrow \delta$ PT based on a phenomenological (rather than physical) nucleation mechanism.⁹ In Ref. 9 the contribution of nucleation to the rate in the change of the volume fraction was described by the transition state theory¹³ and the first-order thermally activated kinetic equation in the region of stability of the δ phase,

$$\dot{c}_n = (1 - c) = a(1 - c),$$

$$p(\text{MPa}) < -775.139 + 1.794\theta(\text{K}), \quad (24)$$

$$a = \frac{k\theta}{h} \exp\left[\frac{\theta S_n - H_n - np\Delta v_{\beta-\delta}}{R\theta}\right], \quad (25)$$

where H_n and S_n are the enthalpy and entropy of nucleation, respectively, n is the factor that determines the transformation work of nucleation (in Ref. 9, where the effect of pressure was not analyzed, it was assumed that $n=1$). For comparison, in Refs. 5 and 6 nucleation was considered as a reversible process which resulted in an additional term in Eq. (24). This leads to the existence of a stationary value of $c < 1$ for high temperatures (and pressures) when the contribution of nucleation to the overall kinetics prevails, which is

physically contradictory. In contrast, use of Eq. (24) leads to complete PT.

Additive combination of Eq. (24) with the kinetic Eq. (1) for the growth stage based on the virtual melting results in the following overall kinetics:

$$\dot{c} = \dot{c}_n + \dot{c}_g = a(1 - c) + bc(1 - c). \quad (26)$$

Solution to differential equation Eqs. (26) for fixed a and b and initial condition $c(0)=0$ is as follows:

$$c = \frac{a(e^{(a+b)t} - 1)}{b + ae^{(a+b)t}}. \quad (27)$$

From the condition $c=0.5$, one can find the time to half conversion, which was used in Refs. 5 and 6 to compare with experiment. We obtained

$$t = \frac{\ln\left(2 + \frac{b}{a}\right)}{b + a}. \quad (28)$$

Three parameters in Eqs. (25) and (2), $H_n = 309.328$ kJ/mole, $S_n = 374.239$ J/mole K, and $Z = 5.7 \times 10^{-12}$ (note that Z is the same as in current model; see Table II) were determined from the best fit of experimental data on time for half of the transformation for $\beta \rightarrow \delta$ PT.^{5,6}

Equations (27) and (28) adequately describe experimental data on time for half of the transformation and individual kinetic curves under various temperatures for the $\beta \rightarrow \delta$ PT under isothermal conditions at ambient pressure.⁹ However, our attempt to apply Eq. (26) to the problem of PT in a rigid cylinder that involves high pressure and eventual cyclic $\beta \leftrightarrow \delta$ PTs in the vicinity of the phase equilibrium line exhibits a number of contradictions. First, the nucleation term is not consistent with the thermodynamics, so there is an increase in the δ -phase concentration even if the pressure increases (due to, for example, volumetric expansion during the PT) shifting the pressure-temperature trajectory into the region of stability of the β phase. If we do not allow this by multiplying \dot{c}_n in Eq. (26) by $H(-775.139 + 1.794\theta - p)$, where $H(x)$ is the Heaviside unit step function [i.e., $H(x) = 1$ for $x \geq 0$ and 0 for $x < 0$], then the solution exhibits strong oscillations in \dot{c} . Indeed, at high pressure, the PT temperature is also high and the term \dot{c}_n is large. When the pressure-temperature trajectory shifts into the region of stability of the β phase due to volume and pressure increase, \dot{c}_n jumps to zero. Lack of the transformation expansion combined with pressure decrease due to HMX decomposition and gas leaking shifts the pressure-temperature trajectory back into the region of stability of the δ phase and the jump of \dot{c}_n to the large value and so on.

Without the Heaviside function, noncontradictory results can be obtained for a large fitting parameter, $n \approx 20$, suppressing nucleation kinetics under high pressure. Then, the nucleation term is getting small enough and the reverse PT is observed in most cases in the region of stability of the β phase. However, this does not guarantee that for slightly different regimes new contradictions will not appear. This does not happen when we use the fully physically based model, Eqs. (1)–(3). Consequently, despite the fact that both physical and phenomenological models describe isothermal ex-

periments at zero pressure equally well, a fully physically based model has significant advantage in comparison with a phenomenological model because of this validity over much broader regimes.

V. CONCLUDING REMARKS

In this paper, numerical analysis of the heating of PBX 9501 with a constant rate inside of a rigid cylinder is performed. The coupled continuum thermo-mechanochemical model developed in Ref. 1 is used. The model includes the physically based kinetics of the $\beta \leftrightarrow \delta$ PTs in crystalline HMX, and phenomenological kinetics of chemical decomposition of the HMX and binder (leading to gas formation), as well as gas leaking from the cylinder. The mechanical part of the model takes into account elastic, thermal, and transformational straining, as well as straining due to mass loss. The effect of the heating rate, initial porosity and prestraining, HMX and binder decomposition, as well as gas leaking rule on the kinetics of the $\beta \leftrightarrow \delta$ PT and pressure buildup, is analyzed numerically. The methods to control the $\beta \rightarrow \delta$ PT by controlling the process parameters are enumerated at the end of Sec. III. The obtained results on the prediction of the thermo-mechanochemical behavior of HMX within PBX 9501 under various temperature-pressure loading histories in a pre-ignition regime is of significant importance for the safety of its storage, transportation, and handling, and development of more comprehensive ignition models. Our models can be used to improve models aimed at predicting time to explosion.^{10,11,14,15} Multiple kinetic parameters for each reaction step in HMX and the binder in those models were chosen to obtain the best fit to time-to-explosion versus temperature experimental data. Incorporation of more precise and physically based kinetic equations for $\beta \leftrightarrow \delta$ PTs, and calibration of one of the steps of HMX and binder decomposition using thermogravimetric data (i.e., mass loss) reduces the number of kinetic parameters to be fitted to time-to-explosion versus temperature experiments. Alternatively, kinetic equations for additional decomposition steps, neglected here, and corresponding reaction heats can be added to our model.

One direction of further development is to incorporate pressure into the kinetic equation for the HMX and binder decomposition.

Note that the knowledge of the suggested nucleation mechanism can be used to activate similar mechanisms for other PTs, especially with a large volumetric strain and interface energy. This will allow a reduction of the PT pressure and temperature by substituting a direct solid-solid PT by a cluster-cluster PT in a proper liquid medium. It will also allow the discovery of phases previously hidden due to large volumetric strain and interface energy which cannot appear by a direct solid-solid PT. For example, α HMX is stable at $382.4 < \theta < 430$ K; however, β HMX does not transform to α in this temperature range; it transforms to δ at $\theta > 432$ K. In the presence of various solvents, α HMX appears at $382.4 < \theta < 430$ K.¹⁶ Furthermore, by a proper choice of solvent, one can nucleate and grow the desired

metastable phase, if the change of the interface energy during cluster-to-cluster PT for this phase is significantly smaller than for the stable phase.

On the other hand, in the HMX crystals without a binder, nucleation occurs at the specific nucleating defects, which may be inclusions of the solvent used in HMX synthesis¹⁷ or some stress concentrators. Nucleation temperature varies in a wide range from crystal to crystal because of the different potencies of nucleation sites. For example, in Ref. 8 the $\beta \rightarrow \delta$ PT was not observed below 448 K. The case without the nitroplasticizer is not relevant for the current paper. However, it is relevant for the case when the nitroplasticizer disappears before the nucleation of the δ phase.

The virtual melting transformation mechanism is also expected to be the main mechanism of pressure-induced crystal-crystal and crystal-amorphous PTs for a broad class of materials.¹⁸ They occur in materials with the specific pressure-temperature phase diagram when the melting temperature of one of the phases reduces with growing pressure. This mechanism is expected in the amorphization of ice, α -quartz, coesite, jadeite, polymet, Ge and Si, BN and graphite.

ACKNOWLEDGMENTS

V.I.L. acknowledges the LANL contracts (13720-001-05-AH and 31553-002-06) and NSF grants (CMS-02011108 and CMS-0555909); B.F.H., L.B.S., and B.W.A. acknowledge the support of the Laboratory Research and Development and H.E. Science Programs at Los Alamos National Laboratory. The main part of this work has been performed

during V.I.L.'s sabbatical leave at LANL. The hospitality of L.B.S., B.F.H., B.W.A., and D.K.Z. is very much appreciated.

- ¹V. I. Levitas, B. F. Henson, L. B. Smilowitz, D. K. Zerkle, and B. W. Asay, *J. Appl. Phys.* **102**, 113502 (2007).
- ²V. I. Levitas, L. B. Smilowitz, B. F. Henson, and B. W. Asay, *Appl. Phys. Lett.* **89**, 231930 (2006).
- ³V. I. Levitas, B. F. Henson, L. B. Smilowitz, and B. W. Asay, *Phys. Rev. Lett.* **92**, 235702 (2004).
- ⁴V. I. Levitas, B. F. Henson, L. B. Smilowitz, and B. W. Asay, *J. Phys. Chem. B* **110**, 10105 (2006).
- ⁵B. F. Henson, L. B. Smilowitz, B. W. Asay, and P. M. Dickson, *J. Chem. Phys.* **117**, 3780 (2002).
- ⁶L. B. Smilowitz, B. F. Henson, B. W. Asay, and P. M. Dickson, *J. Chem. Phys.* **117**, 3789 (2002).
- ⁷B. F. Henson, B. W. Asay, R. K. Sander, S. F. Son, J. M. Robinson, and P. M. Dickson, *Phys. Rev. Lett.* **82**, 1213 (1999).
- ⁸A. K. Burnham, R. K. Weese, and B. L. Weeks, *J. Phys. Chem. B* **108**, 19432 (2004).
- ⁹V. I. Levitas, L. B. Smilowitz, B. F. Henson, and B. W. Asay, *J. Chem. Phys.* **124**, 026101 (2006).
- ¹⁰A. P. Wemhoff, A. K. Burnham, and A. L. Nichols, *J. Phys. Chem. A* **111**, 1575 (2007).
- ¹¹J. J. Yoh, M. A. McClelland, J. L. Maienschein, A. L. Nichol, and C. M. Tarver, *J. Appl. Phys.* **100**, 073515 (2006).
- ¹²S. Wolfram, *The Mathematica Book*, 5th ed. (Wolfram Media/Cambridge University Press, Cambridge, 2003).
- ¹³G. G. Hammes, *Principles of Chemical Kinetics* (Academic, New York, 1978).
- ¹⁴C. M. Tarver, *J. Energ. Mater.* **22**, 93 (2004).
- ¹⁵C. M. Tarver and T. D. Tran, *Combust. Flame* **137**, 50 (2004).
- ¹⁶H. H. Cady and L. C. Smith, "Studies on the Polymorphs of the HMX," Report No. LAMS-2652, Los Alamos Scientific Laboratory, 1962.
- ¹⁷L. B. Smilowitz, B. F. Henson, M. Greenfield, A. Sas, B. W. Asay, and P. M. Dickson, *J. Chem. Phys.* **121**, 5550 (2004).
- ¹⁸V. I. Levitas, *Phys. Rev. Lett.* **95**, 075701 (2005).